

## Supplementary Information

### **Integrating energy-environmental functions into multifaceted lignocellulose valorization: high-performance supercapacitors and antibiotic decomposition**

Jun Guo<sup>a,1</sup>, Jikun Xu<sup>a,1,\*</sup>, Xiao Xiao<sup>b</sup>, Lin Dai<sup>c</sup>, Chuntao Zhang<sup>a\*</sup>, Kaifu Huo<sup>d</sup>

<sup>a</sup> *Key Laboratory of Hubei Province for Coal Conversion and New Carbon Materials, School of Chemistry and Chemical Engineering, Wuhan University of Science and Technology, Wuhan 430081, China*

<sup>b</sup> *College of Biomass Science and Engineering, Sichuan University, Sichuan 610065, China*

<sup>c</sup> *Tianjin Key Laboratory of Pulp and Paper, Tianjin University of Science and Technology, Tianjin 300457, China*

<sup>d</sup> *Wuhan National Laboratory for Optoelectronics, Huazhong University of Science and Technology, Wuhan 430074, China*

<sup>1</sup> These authors contributed equally to this work.

*\*Corresponding authors*

*E-mail: jkxu@wust.edu.cn (J. Xu); zhangchuntao@wust.edu.cn (C. Zhang)*

## **S1. Experimental section**

### *1.1. Raw materials*

The representative lignocellulose, wheat straw, was harvested from Hubei province (China). The straw was rinsed repeatedly and then desiccated in a drying cabinet at 60 °C for 72 h. The wheat straw is mainly consisted of 41.3% cellulose, 24.6% hemicelluloses, and 19.8% lignin. We used all kinds of chemical reagents in the analytical grade or best available grade without further purification. All of the quantitative experiments are performed in triplicate and the results are presented as the average values.

### *1.2. Hydrothermal pretreatment of wheat straw and xylan-based microspheres*

A typically hydrothermal treatment was carried out in an autoclave. Wheat straw of 10 g and FeCl<sub>3</sub> of 3 g were incipiently immersed in 100 mL deionized water overnight with a solid to liquid ratio of 1:15 (g/mL). Subsequently, the resulted slurry was transferred to a stainless steel autoclave and hydrothermally treated at 180 °C for 1 h. Afterwards, the hydrothermally treated wheat straw was recovered by filtration and dried at 80 °C for 24 h, which served as the precursor for the Co-N-C biochar catalysts. The autohydrolysate obtained after the hydrothermal process was collected to further conduct a hydrothermal carbonization at 200 °C for 12 h in the same autoclave. After the above process, the production of carbon microspheres can be easily isolated *via* vacuum filtration and then freeze-dried to synthesize Fe-N-C microspheres as supercapacitor electrode.

### *1.3. Construction of Fe-N-C microspheres and Co-N-C catalysts*

For the fabrication of Fe-N-C microspheres, 0.5 g of as-prepared carbon microspheres from autohydrolysate, 3 g of  $\text{KHCO}_3$ , and 0.25 g melamine were co-ground for 30 min to reach the uniform blend. Next, the resultant mixture was transferred to a corundum boat and annealed at 800 °C for 1 h in a tubular furnace. In detail, the heating speed was 5 °C  $\text{min}^{-1}$  and the flowing rate of protection gas ( $\text{N}_2$ ) was 120 mL  $\text{min}^{-1}$ . After the reaction, the black solid product was obtained after washing multiple times with 1 M HCl and DI water. Lastly, the above Fe, N co-doped porous carbon microspheres were dried at 105 °C overnight to gain Fe-N-C.

With regard to Co-N-C catalysts, 1 g of hydrothermally treated wheat straw, 3g of cobalt acetate, 6 g of  $\text{KHCO}_3$ , and 0.5 g melamine were also co-ground for 30 min to reach the uniform blend. Afterwards, the resulting mixture was transferred to a corundum boat and annealed at 800 °C for 1 h in a tubular furnace. In detail, the heating speed was 5 °C  $\text{min}^{-1}$  and the flowing rate of protection gas ( $\text{N}_2$ ) was 120 mL  $\text{min}^{-1}$ . After the reaction, the black solid product was obtained after washing multiple times with 1 M HCl and DI water. Finally, the above Co, N co-doped activated carbon were dried at 105 °C overnight to collect Co-N-C.

### *1.4. Analytic procedures*

The morphology, microstructure, elemental analysis, surface chemical states, and specific surface area of Fe-N-C microspheres and Co-N-C catalysts were performed with scanning electron microscope (SEM, ZEISS MERLIN Compact), transmission electron microscope (TEM, FEI Tecnai G2 F20), X-ray diffraction (XRD), X-ray

photoelectron spectroscopy (XPS), Raman spectroscopy and nitrogen adsorption-desorption isotherms respectively. The surface morphology of the prepared materials was observed by high angle annular dark-field scanning TEM (HAADF-STEM) images and corresponding elemental mapping were achieved by FEI Titan G2 80–200 TEM/STEM. XRD patterns were collected on a Rigaku MiniFlex 600 instrument. X-ray photoelectron spectroscopy (XPS) measurements were carried out on a Kratos spectrometer at room temperature to analyze the surface chemical states. Nitrogen adsorption-desorption isotherms were carried out using automatic specific surface area and porosity analyzer (JWBK122W, JWGB Ltd., China), and analyzed with Brunauer–Emmett–Teller (BET) model.

For electrochemical measurements of Fe-N-C microspheres electrode, synthesizing the working electrodes of  $1.0 \times 1.0 \text{ cm}^2$  is a universal procedure. In brief, Fe-N-C microspheres (80 wt %), conductive carbon black (10 wt %), and polyvinylidene fluoride (PVDF, 10 wt %) were uniformly dispersed in N-methyl-2-pyrrolidone (NMP) by sufficient grinding. The resulting slurry was then coated onto a cleaned nickel foam (battery-grade,  $1 \text{ cm}^2$ ) evenly and vacuum-dried at  $60 \text{ }^\circ\text{C}$ . The weight of the material on a single electrode was approximately 2 mg after compressing. For the three-electrode setup, Pt wire and Hg/HgO electrodes served as counter and reference electrodes in 6.0 M KOH. All of the electrochemical measurements were carried out in a CHI760E workstation. The capacitance ( $C_g, \text{F g}^{-1}$ ) in the three-electrode setup can be calculated

from the equation of  $C_g (\text{F g}^{-1}) = \frac{I\Delta t}{m\Delta v}$  (where  $I$ ,  $\Delta t$ ,  $m$ , and  $\Delta v$  represent the current (A), discharge time (s), the material weight on a single electrode, and the discharge

potential excluding the *IR* drop (*V*), respectively).

The catalytic performance of as-prepared Co-N-C catalysts was investigated at room temperature (25 °C) by mixing target pollutant (tetracycline), catalyst and PDS. The reaction solution was evenly stirred by a magnetic stirrer and the initial pH of reaction solution was not adjusted. The 3 mL of the sample was extracted at a certain time interval and loaded into a quartz cuvette for UV–vis spectrophotometer analysis *via* a 0.22 μM millipore filter to quantify the concentration of tetracycline. Without heat-regeneration, the Co-N-C catalysts were recycled after each degradation process by centrifuged, washed three times with water and dried overnight at 60 °C in a vacuum for reusability and stability experiment. In addition, quenching experiments were also studied by adding ethanol (EtOH), tert-butyl alcohol (TBA), *p*-benzoquinone (*p*-BQ), and furfuryl alcohol (FFA) as the quenching reagents to verify the contributions of radicals and non-radicals in the Co-N-C/PDS system. The electron paramagnetic resonance (EPR) spectra were collected using a Bruker A300 spectrometer (EPR, Bruker Biospin GmbH, Rheinstetten, Germany) with 2,2,6,6-tetramethyl-4-piperidinol (TEMP) and 5,5-dimethyl-1-pyrroline N-oxide (DMPO) as the spin-trapping agents. Electrochemical measurement of MBC was performed in a three-electrode cell (CHI 760E, CH Instrument, Shanghai) at 25 ± 2 °C. First-principles calculations were performed using the density-functional-theory (DFT) in the "Vienna Ab initio Simulation Package" (VASP 5.4.1).

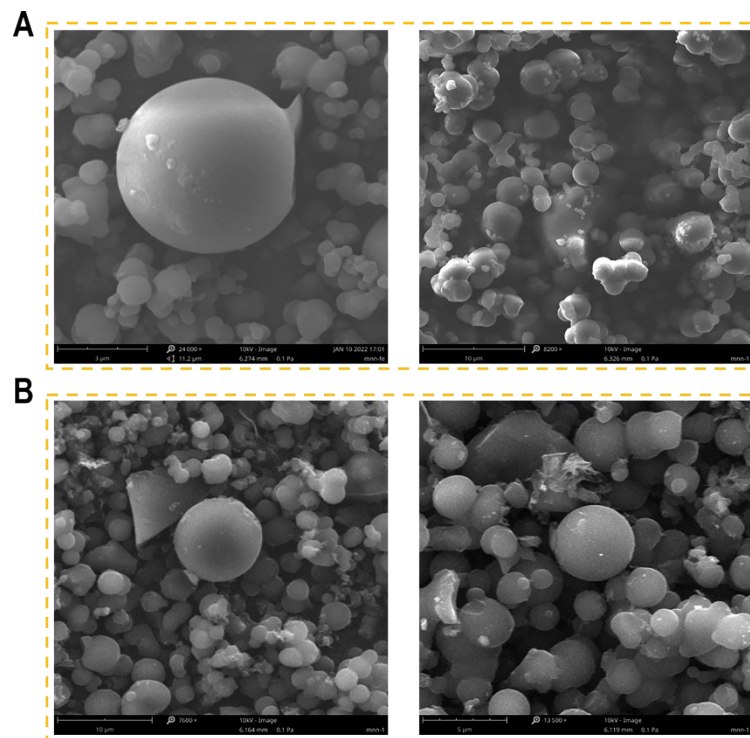


**Figure S1.** Scanning electron microscopy (SEM) images to visualize the microstructures of (A) hydrolysate-based microballoons and (B) Fe-N-C microspheres.

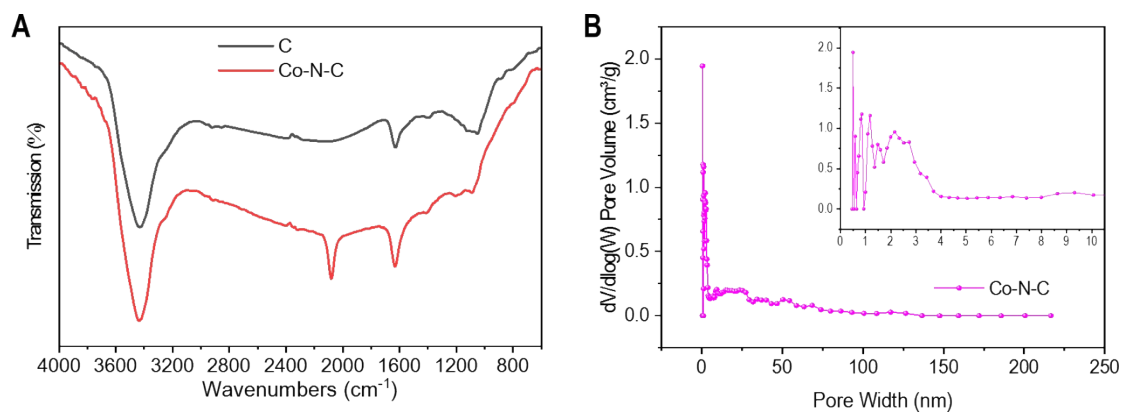


**Figure S2.** (A) Fourier transform infrared (FTIR) spectrum and (B) pore size distribution of Co cluster on N-doped carbon (Co-N-C) from hydrothermal-treated wheat straw.

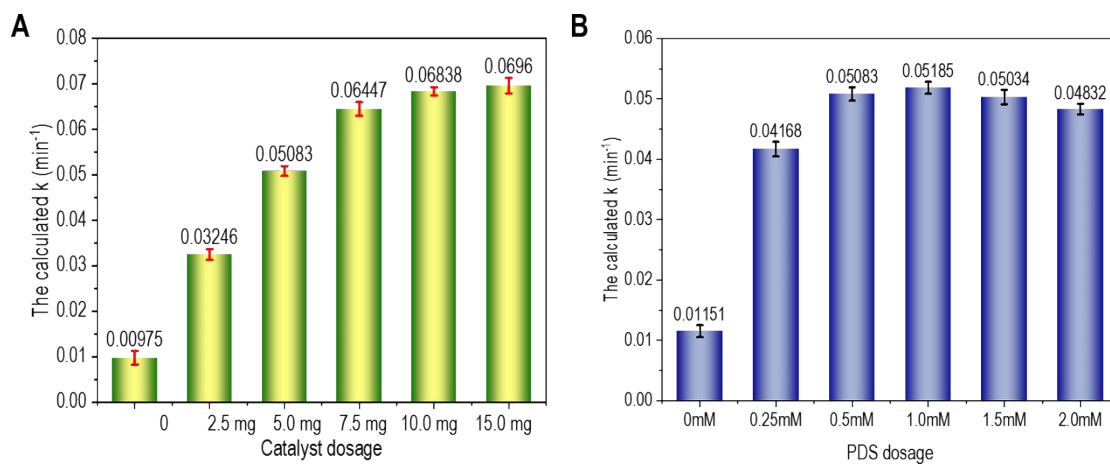


**Figure S3.** The calculated reaction rate constant ( $k$ ) of catalytic tetracycline degradation using Co-N-C mediated PDS activation by varying (A) the catalyst Co-N-C amount and (B) the peroxydisulfate (PDS)- $(\text{NH}_4)_2\text{S}_2\text{O}_8$  dosage.



**Table S1.** Summary of the comparable literatures of lignocellulose-based electrode for supercapacitors.

| Raw materials  | Specific surface area (m <sup>2</sup> g <sup>-1</sup> ) | Capacitance (F/g at 1 A/g) | Recycling stability   | Ref.             |
|----------------|---|----------------------------|-----------------------|------------------|
| Wheat straw    | 892   | 247                        | 97% (10000 cycles)    | 1                |
| Sawdust        | 1281.6  | 152.8                      | 98.3% (5000 cycles)   | 2                |
| Bamboo chips   | 755   | 208                        | /                     | 3                |
| Lignocellulose | 1535  | 193.6                      | 97.9% (10000 cycles)  | 4                |
| Cotton         | 584   | 198.3                      | 95.4% (6000 cycles)   | 5                |
| Hemp stem      | 1193  | 255                        | 97.8% (10000 cycles)  | 6                |
| Bamboo         | 1732  | 171.4                      | 95% (5000 cycles)     | 7                |
| Larch sawdust  | 805.91  | 157.07                     | 101.06% (2000 cycles) | 8                |
| Rice straw     | 3333  | 340                        | 93.6% (10000 cycles)  | 9                |
| Corn           | 2305.7  | 338                        | 102.7% (5000 cycles)  | 10               |
| Wheat straw    | 2635  | 305.42                     | 100% (10000 cycles)   | <b>This work</b> |

## References

1. W. Liu, J. Mei, G. Liu, Q. Kou, T. Yi and S. Xiao, *ACS Sustainable Chemistry & Engineering*, 2018, **6**, 11595-11605.
2. G. Lin, Q. Wang, X. Yang, Z. Cai, Y. Xiong and B. Huang, *RSC Advances*, 2020, **10**, 17768-17776.
3. Y. Li, Z. Li, B. Xing, H. Li, Z. Ma, W. Zhang, P. Reubroycharoen and S. Wang, *Journal of Analytical and Applied Pyrolysis*, 2021, **155**, 105072.
4. J. Yi, Y. Qing, C. Wu, Y. Zeng, Y. Wu, X. Lu and Y. Tong, *Journal of Power Sources*, 2017, **351**, 130-137.
5. Y. Liu, Z. Shi, Y. Gao, W. An, Z. Cao and J. Liu, *ACS Applied Materials & Interfaces*, 2016, **8**, 28283-28290.
6. D. Qiu, C. Kang, A. Gao, Z. Xie, Y. Li, M. Li, F. Wang and R. Yang, *ACS Sustainable Chemistry & Engineering*, 2019, **7**, 14629-14638.

7. Y. Gong, D. Li, C. Luo, Q. Fu and C. Pan, *Green Chemistry*, 2017, **19**, 4132-4140.
8. Y. Zhang, J. Sun, J. Tan, C. Ma, S. Luo, W. Li and S. Liu, *Fuel*, 2021, **305**, 121622.
9. H. Jin, J. Hu, S. Wu, X. Wang, H. Zhang, H. Xu and K. Lian, *Journal of Power Sources*, 2018, **384**, 270-277.
10. Z. Xu, X. Zhang, X. Yang, Y. Yu, H. Lin and K. Sheng, *Energy & Fuels*, 2021, **35**, 14157-14168.